Journal of Thermal Analysis and Calorimetry (2019) 136:783–794
https://doi.org/10.1007/s10973-018-7630-z

Pyrolysis of tobacco factory waste biomass

TG-FTIR analysis, kinetic study and bio-oil characterization

Zeynep Yıldız[1] · Selim Ceylan[1]

Received: 20 December 2017 / Accepted: 2 August 2018 / Published online: 17 August 2018

Abstract
Tobacco waste is one of the main industrial agricultural wastes. In this study, potential of pyrolysis process for valorization of this type of biomass waste was investigated based on thermogravimetirc analysis. Thermogravimetric analysis of the tobacco waste material was carried out at different heating rates (5, 10, 20, 40 °C min^{-1}) by heating from room temperature to 900 °C in an inert nitrogen atmosphere. The main decomposition occurred approximately between temperatures 150 and 390 °C. Pyrolysis kinetic was investigated by the DAEM method to determine kinetic parameters (activation energy and frequency factor) by using thermogravimetric data. Activation energy (E) and the frequency factor (k_0) were ranging from 280.38 to 201.96 kJ mol^{-1} and 2.45E+14 to 8.19E+25 s^{-1}, respectively. The evolved gaseous products were investigated by using the TG-FTIR technique, and effect of temperature and heating rate on products was examined. Characterization of the bio-oil obtained from pyrolysis of the tobacco waste in the fixed-bed reactor was carried out using FT-IR, GC–MS and ^{1}H-NMR techniques. According to GC–MS results, bio-oil consists mainly of nicotine (26.78%), phenol (8.02%) and limonene (4.59%) compounds. GC–MS, FT-IR and ^{1}H-NMR results were consistent with each other.

Keywords Tobacco waste · Biomass · Pyrolysis · Distributed activation energy model · TGA-FTIR

Introduction

The enormous consumption of fossil fuels, depletion of energy resources and serious environmental pollution are major problems related with fossil fuel usage that lead researchers focus on alternative energy sources. Demand for clean and renewable energy sources is increasing day by day[1–3]. Biomass is a clean, cost-effective, abundant carbon-containing, low-sulfur containing renewable material used for heat and fuel production. At the same time, biomass is among the fourth largest sources of energy that meet more than 14% of world energy needs [4, 5]. The biomass can be converted into valuable products when applied to a variety of conversion processes [6]. Pyrolysis is the thermochemical conversion process applied under an inert nitrogen atmosphere [7–9].

After the processing of the tobacco used in the production of cigarettes, approximately 20% of the residue remains. A large amount of tobacco residues represents the significant amount of biomass to be treated. Thanks to the pyrolysis method, renewable materials such as tobacco waste can be converted into valuable products (such as bio-char, bio-oil and biogas). [10–12]. A number of studies have been published in the literature on pyrolysis of tobacco wastes. Cardoso et al. [13] investigated pyrolysis of tobacco waste using thermogravimetric analysis technique. Wu et al. [14] investigated kinetics and reaction chemistry of pyrolysis and combustion of tobacco waste. They applied iso-conversional methods and calculated activation energies. Chen et al. [15] investigated pyrolysis of tobacco waste and investigated bio-oil composition and nitrogen conversion degree to obtain optimum pyrolysis conditions. Gao et al. [10] applied model-fitting method to analyze reaction kinetics of tobacco waste pyrolysis to obtain kinetic triplets. Wang et al. [16] investigated pyrolysis and combustion profiles and kinetics of

✉ Zeynep Yıldız
zeynepyildiz.omu@gmail.com

[1] Department of Chemical Engineering, Engineering Faculty, Ondokuz Mayıs University, 55139 Samsun, Turkey

tobacco waste using DAEM model. Cordoso and Ataide [11] reported on the effects of temperature and inorganic content on pyrolysis of tobacco residues. Hossain et al. [17] studied to optimize pyrolysis reactor conditions to produce nicotine. These studies are generally sole kinetic or product characterization studies. However, this study is a comprehensive study that brings kinetic analysis and detailed product analysis to present a detailed report on tobacco waste pyrolysis process.

Kinetic study is very useful for understanding degradation mechanisms, reaction rate and reaction parameters. It can facilitate the design, operation and optimization of the operating conditions of the reactors [18]. There are many models in the literature such as Kissinger model, Flynn–Wall–Ozawa (FWO) model, Friedman (FR) model, Coats–Redfern model and distributed activation energy model (DAEM) for calculation of pyrolysis kinetics. Among these models, the distributed activation energy model (DAEM) is widely used for the analysis of complex reactions during pyrolysis of many biomasses [19, 20].

Thermochemical processes play an important role in the conversion of biomass materials to energy. Thermogravimetric analysis (TGA) is one of the general techniques used to determine kinetic parameters during biomass pyrolysis and to examine thermal behaviors [20, 21]. TGA is the technique in which sample mass is measured as a function of time or temperature in nitrogen or air atmosphere. The reduction in sample mass in the TGA technique reflects physical and chemical changes throughout the conversion. Differential thermogravimetric curves (DTG) are used to clarify various thermogravimetric processes [22].

In this study, pyrolysis behaviors of tobacco waste were investigated using thermogravimetric data at different heating rates (5, 10, 20 and 40 °C min^{-1}). The kinetic parameters (E and k_0) for the pyrolysis process were estimated using the distributed activation energy model (DAEM) method. Techniques such as FT-IR, XRF, proximate and ultimate analyses were preferred for the characterization of raw tobacco waste, while TG-FTIR analysis identified volatile products that were evolved during pyrolysis of the tobacco waste. At the same time, characterization of the bio-oil obtained from pyrolysis of the tobacco waste at 600 °C in the fixed-bed reactor was carried out using FT-IR, GC–MS and ^{1}H-NMR techniques. FT-IR and ^{1}H-NMR results of the products obtained according to GC–MS results were examined.

Materials and methods

Tobacco waste characteristics

The tobacco wastes (TW) were supplied from a local company in Samsun, Turkey. The samples were washed with deionized water to remove surface dirt and dried in a 100 °C oven overnight. Dried samples were crushed and sieved into a particle size of 63–125 μm to prevent heat and mass transfer limitations in thermogravimetic analysis. TW were characterized in terms of proximate and ultimate analysis, according to the ASTM standards (E871, D1102-84) by using a programmable ash oven. Leco type analyzer CHNS-932 was used for the elemental analysis and oxygen bomb calorimeter was used for the determination of high heating value of TW. For XRF analysis, TW samples were dried in an incubator and then grounded in Spex mill. The obtained powder was sieved using a 140-mesh sieve and then stirred for 25 min. Then, samples were pressed into 40-mm-diameter pellets. The measurement parameters were set up by using the Epsilon 5 EDXRF system's inbuilt software. Samples were irradiated by X-rays from Gd tube under a vacuum equipped with a liquid nitrogen cooled PAN-32 Ge X-ray detector having window thickness of 8 μm. The power, current and high voltage of the instrument was 600 W, 6 mA and 100 kV, respectively.

Thermogravimetric analysis (TG)

Thermogravimetric analysis (TGA) was carried out using simultaneous differential thermogravimetric analyzer (DTA) equipped with a heat flux-type DTA and a TGA (Shimadzu, DTG-60, Japan; with a precision of temperature measurement ± 0.1 K, DTA sensitivity ± 0.1 μV and microbalance sensitivity ± 0.1 μg) at heating rates of 5, 10, 20 and 40 °C min^{-1} under a nitrogen atmosphere with a flow rate of 100 mL min^{-1} with samples of approximately 10 mg.

TGA-FTIR analysis

The TGA–FTIR experiments were carried out in a thermogravimetric analyzer coupled with Fourier transform infrared spectrometry (Perkin Elmer Simultaneous Thermal Analysis (SDTQ) 600). Approximately 10 mg of TW was loaded onto the sample holder for each run. The samples were heated from ambient temperature to 800 °C at a heating rate of 5, 20 and 40 °C min^{-1}. The flow cell connecting the TG and FTIR was heated to 200 °C to prevent the produced gas from condensing on the cell wall [23]. The flow rate of the carrier inert nitrogen gas was 100 mL min^{-1}. The spectral region of the FT-IR was 4000–400 cm^{-1}, and spectrum scan was conducted with 0.12-s intervals.

Kinetic analysis

In kinetic parameters of TW, pyrolysis process was investigated by using DAEM method. The DAEM

represented is as follows when it is applied to represent the change in total volatiles [20].

$$1 - V/V^* = \int_0^\infty \exp\left(\frac{k_0}{a}\int_0^T e^{-E/RT}dT\right) f(E)dE \quad (1)$$

where V is the volatile content at temperature T, V^* is the effective volatile content, k_0 is the frequency (or pre-exponential) factor, E the activation energy, T the absolute temperature, R the universal gas constant. The distribution curve $f(E)$ is defined to satisfy

$$\int_0^\infty f(E)dE = 1. \quad (2)$$

Equation (1) can be simplified to Eq. (3)

$$V/V^* = 1 - \int_{E_s}^\infty f(E)dE = \int_0^{E_s} f(E)dE \quad (3)$$

where E is the activation energy at a given temperature. The simplified DAEM model can be given as Eq. (4).

$$\ln\left(\frac{\beta}{T^2}\right) = \ln\left(\frac{k_0 R}{E}\right) + 0.6075 - \left(\frac{E}{RT}\right). \quad (4)$$

In Eq. (4), β is heating rate, T is absolute temperature (K), k_0 pre-exponential factor, R is universal gas constant and E is the activation energy. In the plot of the natural ln (β/T^2) versus inverse temperature, $1/T$, at selected conversion values, slope of straight lines give E.

Pyrolysis experiment

Pyrolysis of 10 g of weighed tobacco waste biomass was carried out in an electrically heated "pyrolysis reactor" with a volume of 600 cm^3. Pyrolysis experiments were carried out under an inert nitrogen gas atmosphere at a flow rate of 100 mL min^{-1} at a temperature of 600 °C with a heating rate of 20 °C min^{-1}. The reactor temperature was supplied by the heat couple placed inside the reactor from the top of the furnace. After the reaction temperature was reached, it was held at 600 °C for 120 min. The liquid products were condensable in the system and captured with dichloromethane (DCM). The solvent (DCM) was separated from the bio-oil using a rotary evaporator, and the resulting bio-oil was characterized.

Gas chromatography–mass spectrometry (GC–MS)

Analysis of the examined pyrolysis products was performed on a gas chromatography–mass spectrometry (GC–MS, Agilent) using FID detector. The GC separation of pyrolysis vapors was performed with a RTX-5 column (30 m × 0.25 mm ID × 0.25 μm) with helium carrier gas flow of 2 mL min^{-1} and a 1:20 split ratio. The temperature of the column was programmed as follows: (1) 80 °C; (2) from 80 to 200 °C at a rate of 10 °C min^{-1}; (3) the column final temperature was maintained at 300 °C for about 10 min.

^{1}H NMR spectroscopy

^{1}H NMR spectra were recorded on 600 MHz Bruker spectrospin instruments. The bio-oil from the pyrolysis of the tobacco waste was diluted with D_2O. Tetramethylsilane (TMS) was used as the standard substance.

Results and discussion

Characterization of TW

The proximate, ultimate analysis and higher heating value of tobacco waste are given in Table 1. The volatile matter content of tobacco waste was 70.20% comparable with previously published biomass species. High volatile matter content was desired in a pyrolysis process to obtain high amount of liquid (bio-oil) and gas products. As seen from Table 1, the ash content of tobacco waste samples was higher than the ash content of other terrestrial biomass [14]. Ash can limit heat and mass transfer while creating problems such as slagging and fouling in boilers. However, there were previously published studies emphasizing the catalytic effect of various minerals (especially alkali metals) in ash that can improve product yields. XRF result of tobacco waste is given in Fig. 1 showing that TW was rich in K and C had positive effect in thermochemical conversion processes [24]. According to the ultimate analysis results, TW had low S content. The S content was critical due to environmental issues such as SO_2 gas emissions and acid rains. The N content of TW was generally high. Nitrogen-related emissions in gas or species in bio-oil content were important for environmental issues. Co-valorization with other biomass types or fossil fuels such as coal can reduce nitrogen release caused by TW.

The FT-IR spectrum of raw TW is shown in Fig. 2 with bands assigned summarized in Table 2. The large peak at 3281 cm^{-1} was attributing to the stretching of primarily O–H groups. The symmetric and asymmetric stretching vibration associated with the peaks at 2918–2847 cm^{-1} of C single bond H were alkyl and aliphatic chains. Moreover, the C=O group was mainly from the acids, aldehydes and ketones [25]. The stretch of C=O in FT-IR spectrum of raw TW was 1603 cm^{-1}, respectively. The 1410–1315 cm^{-1}

Table 1 Proximate and ultimate analysis of TW

	TW (This study)	Tobacco stem (Yang et al. [12])	Tobacco waste (Wu et al. [14])	Cotton husk (Bhavanam and Sastry [20])	White pine (Chiodo et al. [8])	Pine sawdust (Hu et al. [30])
Proximate analysis/mass%/dry, ash-free basis						
Moisture	2.83	3.51	4.31	7.90	7.6	4.54
Ash	17.60	21.70	19.88	6.00	0.80	1.69
Volatile matter	70.20	68.64	59.75	66.00	74.20	82.18
Fixed carbon[a]	9.37	6.14	16.06	20.10	17.40	16.13
Ultimate analysis/mass%/dry, ash-free basis						
C	36.21	32.66	46.96	46.88	45.46	46.36
H	5.14	5.66	5.92	4.83	5.32	5.75
N	2.32	3.81	3.55	0.93	0.18	2.26
S	0.04	0.76	0.66	0.36	0.05	0.32
O[a]	56.27	31.91	42.91	41.00	40.60	43.62
Higher heating value/ MJ kg^{-1}	14.77	11.30	13.88	17.34	17.96	16.81

[a]Calculated by difference

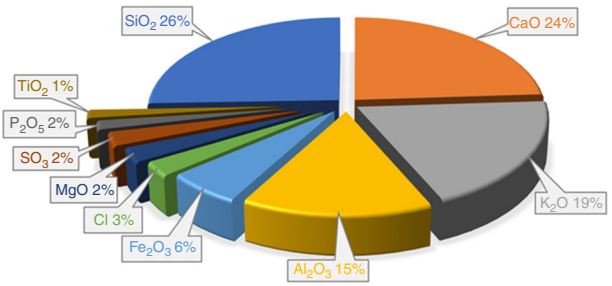

Fig. 1 Chemical composition of TW, mass/%

C–H bending bands correspond to alkyl and aliphatic bending modes [26]. The stretching associated with the peaks at 1323 and 1320 cm^{-1} of raw TW materials was likely indicative of C–O stretching vibration in organic acids, ketones, ethers and alcohols groups [27]. The absorbance peaks at 1025 cm^{-1} were likely the C–O–H deformation in secondary and primary alcohols or aliphatic ethers and lipids [28].

Thermal behavior

The mass/% (TG) and derivative mass/% min^{-1} (DTG) curves of the thermal decomposition of TW at four heating rates, 5, 10, 20 and 40 °C min^{-1} under nitrogen atmosphere are shown in Fig. 3. DTG curves were used to determine the mass loss steps in the pyrolysis process of tobacco waste. Moisture was removed by heating the tobacco waste sample from room temperature to 120 °C. As seen in Table 3, the decomposition range of the tobacco waste sample was determined as approximately 150–400 °C from DTG curves in all heating rates (5, 10, 20

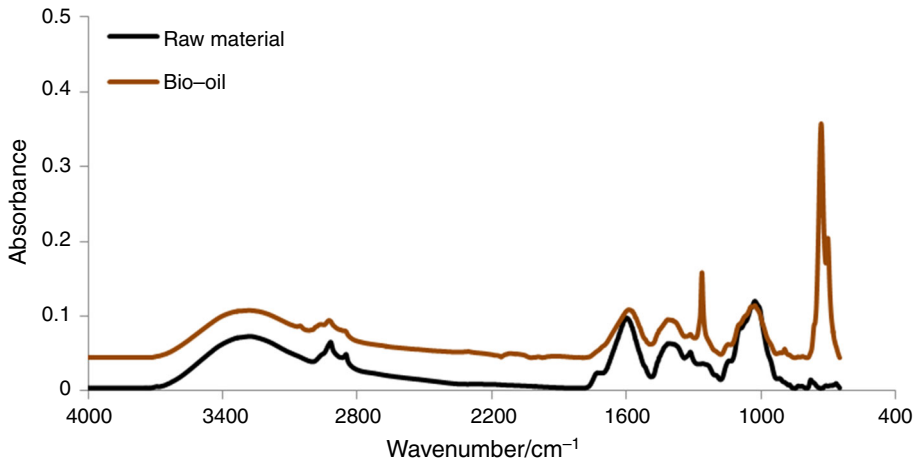

Fig. 2 FT-IR spectra of TW, its bio-oil obtained at 600 °C for 20 °C min^{-1}

Table 2 Functional groups as assigned to specific wave numbers for FT-IR analysis of TW and of bio-oil obtained at 600 °C for 20 °C min^{-1}

Functional group	Vibrational mode	Wave number/cm^{-1}	Assigned species
Functional group of raw TW			
O–H	Stretch	3281	H_2O
C–H	Stretch	2918–2847	Alkyl, aliphatic hydrocarbons
C=O	Stretch	1603	Aldehydes, ketones, acids
C–H	Bending	1410–1315	Alkyl, aliphatic groups
C–O, C–O–H	Stretch	1025	Ethers, alcohols, phenols
Functional groups in devolatized gases from TW			
O–H	Stretch	3400–3900	H_2O
C–H	Stretch	3200–2850	CH_4
C=O	Stretch	2400–2250	CO_2
C–O	Stretch	2250–2000	CO
C=O	Stretch	1900–1650	Aldehydes, ketones, acids
C–O	Stretch	1200	Ethers, alcohols, phenols
Functional groups of bio-oil obtained at 600 °C for 20 °C min^{-1}			
O–H	Stretch	3277	H_2O
C–H	Stretch	2925–2855	Alkyl, aliphatic hydrocarbons
C–H	Stretch	3040	Aromatic hydrocarbons
C=O	Stretch	1590	Aldehydes, ketones, acids
C–H	Bending	1416	Alkyl, aliphatic groups
C–O, C–O–H	Stretch	1028–1264	Ethers, alcohols, phenols

and 40 °C min^{-1}). The main decomposition stages of tobacco waste were observed as peaks in DTG curves. At higher heating rates, difference in temperatures between sample and furnace causes a delay in decomposition. Thus, with increase in heating rate, maximum decomposition rates and temperatures were shifted to higher regions. As seen Fig. 3, maximum decomposition was observed at 40 °C min^{-1}, respectively.

In the DTG curves, the main decomposition step consisting of the anterior and posterior shoulder blades was observed. The anterior shoulder may be thought to be the pyrolysis of hemicellulose. The hemicellulosic decomposition temperature was between 219 and 290 °C. The second peak observed at higher temperatures relates to cellulose decomposition, which had more rigid and stable structure than hemicellulosic. Decomposition of cellulose was reported to occur between 269 and 388 °C. The wide peak indicated the degradation of lignin, the most resistant component of lignocellulosic biomass. Although decomposition of lignin occurred at higher temperatures than other components, the decomposition reactions of these components progress at the same time. The results were consistent with previous studies on wheat stalks, sugar bagasse, corn cob, pine wood, rice husk [26–31].

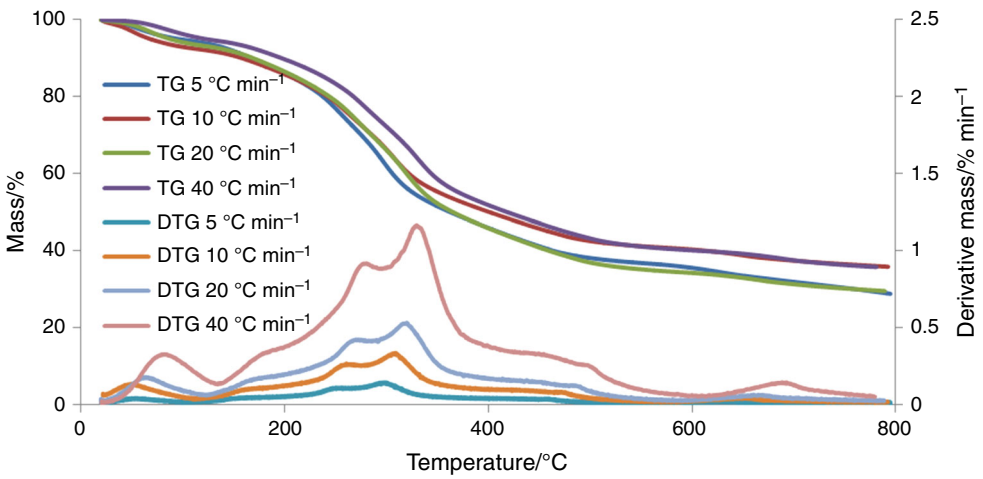

Fig. 3 **a** TG and **b** DTG curves for pyrolysis of TW at different heating rates 5, 10, 20 and 40 °C min^{-1}

Table 3 Thermal decomposition characteristics of TW at different heating rates

Heating rate/°C min^{-1}	T_i/°C	T_f/°C	DTG_{max}/% min^{-1}	T_{max}
5	153	352	1.6	285
10	155	372	2.6	293
20	162	370	6.1	307
40	173	386	11.9	323

T_i initial decomposition temperature, T_f final decomposition temperature, T_{max} temperature at the maximum rate of mass loss, DTG_{max} maximum mass loss rate

Kinetic study

Distributed activation energy model (DAEM) was used to predict kinetic parameters for pyrolysis processes [32]. In this study, pyrolysis of tobacco waste was carried out under an inert nitrogen atmosphere at four different heating rates (10, 20, 30 and 40 °C min^{-1}) to calculate the activation energy (E) and the frequency factor (k_0). The graphs were drawn using thermogravimetric analysis data at different heating rates and presented in Fig. 2. According to the DAEM method, the activation energy (E) and the frequency factor (k_0) values for each conversion rate were calculated using the equation presented in Eq. (4) and the pilot curves plotted in Fig. 4. The E and k_0 values calculated for the pyrolysis of the tobacco waste varied between 201.96 and 280.38 kJ mol^{-1} and 10^{14}–10^{25}, respectively. The mean activation energy value of tobacco waste was 241.27 kJ mol^{-1}. The change in activation energy and frequency factor for each conversion rate is given in Fig. 5.

As can be seen in Fig. 5, the highest activation energy (E) for tobacco waste was calculated to be 280.38 kJ mol^{-1} for a conversion rate of 0.3 and then decreased from 0.3 to 0.8 to 201.96 kJ mol^{-1}. The change in the reaction mechanism caused a change in the activation energy (E) values against the progressive conversion rate. Kinetic parameter calculations for pyrolysis processes were performed by many researchers using DAEM [30–35]. Activation energy (E) is one of the most important parameters used for kinetic models. The activation energies of different biomass samples were examined and presented according to the literature results in recent years in Table 5. Goldfarb and Ceylan [33], Zhang et al. [34] and Wang et al. [35] examined the kinetic mechanism of cocoa bean shells, corn stover and eucalyptus and calculated the average E values as 256.23, 200.00 and 198.58 kJ mol^{-1}, respectively. In general, E values calculated for tobacco waste were similar to those reported in these studies. Table 4 showed that the average activation energy values of the biomass samples were changing between 198.58 and 256.23 kJ mol^{-1} using the DAEM. The average activation energy value (241.27 kJ mol^{-1}) of the calculated tobacco made it as important as the potential biomass fuels.

TGA-FTIR analysis

The TGA-FTIR method was used to determine the functional groups of volatile products released during the decomposition of the raw materials and components. Figures 6 and 7 showed the FT-IR spectra of different conditions.

Figure 6 represented the IR spectra taken at peak temperatures as observed in the DTG curve obtained at 20 °C min^{-1} and at 195 °C, 300 °C, 388 °C, 633 °C; the assigned peaks correspond to the functional groups detailed in Table 2 according to the literature. When the FT-IR spectra of the tobacco waste were examined, O–H bands around 3400–3900 cm^{-1} are shown in Fig. 6. These indicate the presence of evaporating water, alcohol and phenol. There was C–H stretching in the 2850–3200 cm^{-1} spectral region. When the resulting volatile products were taken into consideration, the peaks seen in this region belong to CH_4. As the temperature increased, the bands seen at 2250–2400 cm^{-1} revealed the presence of CO_2 gas [36]. The flexible C=O vibration bands seen around 1900–1650 cm^{-1} were due to the presence of aldehydes and ketones formed during the pyrolysis of tobacco waste [22]. The (C–O) vibration band around 2250–2000 cm^{-1} indicated the formation of carbon monoxide [37]. The C–H and C–O stretching were bands seen around 1460–1370 cm^{-1} and 1050–1200 cm^{-1} that supported the presence of alkanes and alcohols, respectively [22].

Figure 7 presented the maximum rates of conversion of tobacco waste samples as shown by the DTG curves occurred at 285 and 323 °C for heating rates of 5 and 40 °C min^{-1}, respectively. When the 5 °C min^{-1} (the lowest) and 40 °C min^{-1} (the highest) DTG curves were examined, the IR spectrum corresponding to the T_{max} temperature is shown in Fig. 7. When Fig. 7 was examined, according to FT-IR spectra of TW pyrolyzed at 40 °C min^{-1} and 323 °C, we were observing a violent CO_2 wave. This peak was more intense than the peak of the CO_2 group observed at 285 °C and 5 °C min^{-1}. CH_4 and C=O groups (unlike the other spectrum) were observed in FT-IR spectra of TW at 40 °C min^{-1} and 323 °C.

FT-IR characterization

The bio-oil from the pyrolysis of the tobacco waste at 600 °C was analyzed using FT-IR spectroscopy. The classification of functional groups and compounds in the structure of the bio-oil is listed in Table 2. When the bio-oil spectrum in Fig. 1 was examined, the large peak at 3277 cm^{-1} is O–H stretching vibration due to water.

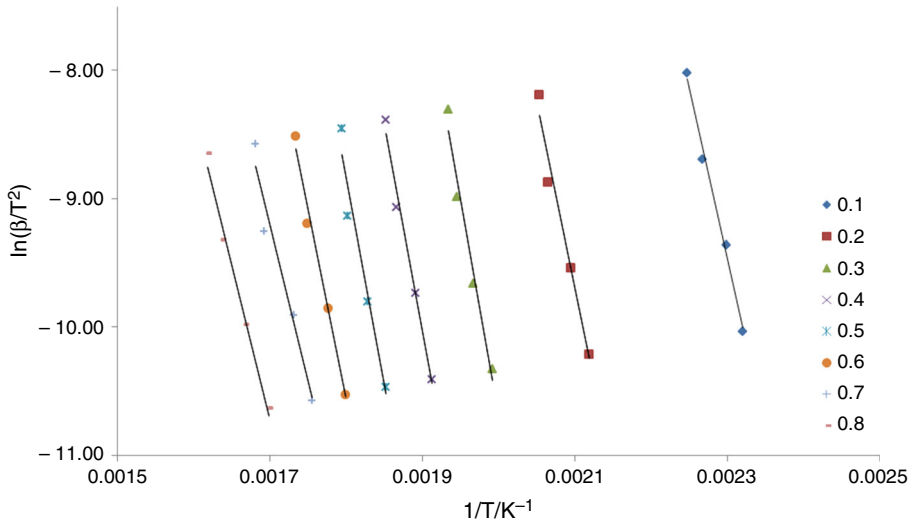

Fig. 4 Isoconversional plot for determination of activation energy of pyrolysis of TW via distributed activation energy model

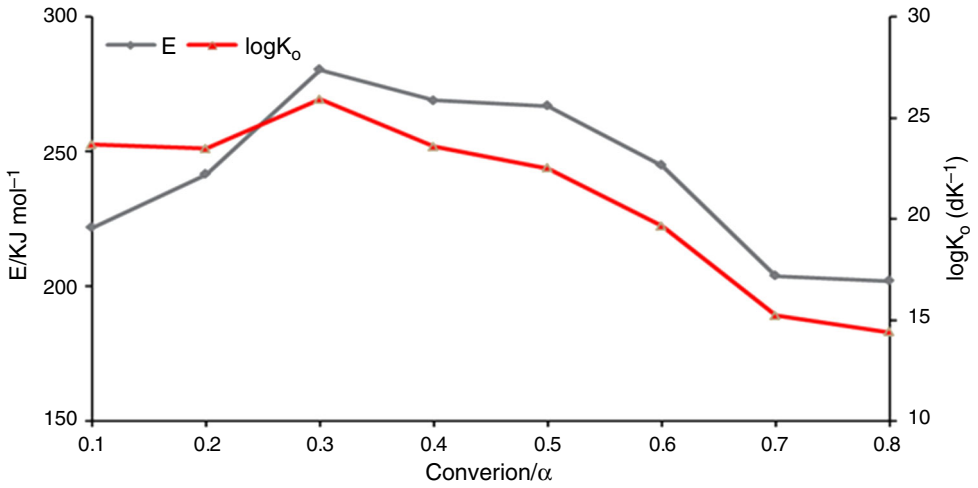

Fig. 5 Activation energy—frequency factor versus conversion relationship

Table 4 Examination of average activation energy of different biomass in literature

Biomass	Average activation energy kJ mol^{-1}	Method	References
Tobacco waste	241.27	DAEM	Present work
Cocoa bean shells	256.23	DAEM	Goldfarb and Ceylan [33]
Corn stover	200.00	DAEM	Zhang et al. [34]
Eucalyptus	198.58	DAEM	Wang et al. [35]

The peaks at 3040 and 2925–2855 cm^{-1}, respectively, were C–H stretching vibrations in the structure of aromatic and aliphatic hydrocarbons. The intensity peak of the C=O asymmetric stretching vibration in the spectrum was observed at 1590 cm^{-1}. This peak showed the presence of acid, aldehyde and ketone compounds and the functionality of the acid compounds consistent with the results of the GC–MS analysis presented in Table 3. Peaks at 1416 cm^{-1} indicated the C–H bending vibration of the aliphatic hydrocarbons and confirm the C–H stretching vibrations [22–27].

GC–MS characterization

GC–MS analysis was performed to determine the organic compounds present in the bio-oil produced under pyrolysis conditions. As can be seen in Fig. 8, the bio-oil produced from tobacco waste was not a very complex mixture and about 70 compounds were detected in the bio-oil product. According to GC–MS results, 17 compounds with a total area of more than 1% were identified and the results are presented in Table 5. The bio-oil consisted of a mixture of 5–28 carbon organic compounds. The bio-oil product was mainly composed of phenols, acids, alkanes and nitrogen-

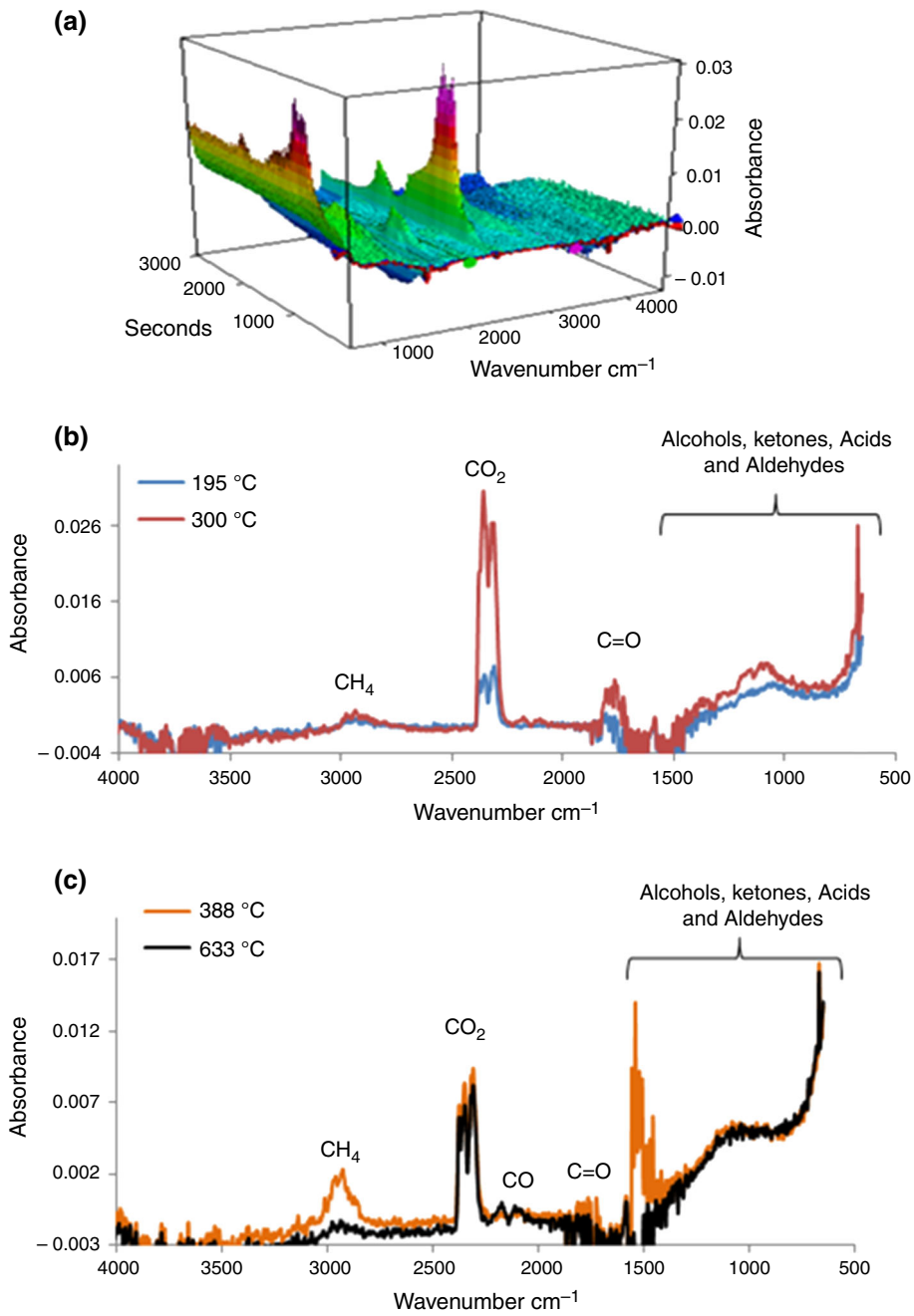

Fig. 6 **a** FT-IR spectra of TW pyrolyzed at 20 °C min^{-1} at **b** 195 °C, 300 °C, **c** 388 °C, 633 °C

containing compounds such as pyridine and nicotine. It was the most abundant nicotine compound with an area of 26.78%. Nicotine and nitrogen-containing compounds are derived from thermal decomposition of the waste tobacco biomass [11]. Compounds with the highest selectivity in the produced bio-oil product, phenol (8.02%), limonene (4.59%) and pentacosane (3.33%) were found to be nicotine (26.78%), respectively. These results showed that bio-oil is consistent with FT-IR and ^{1}H-NMR results.

As shown in the FT-IR results, C–H stretching (3010–3040 cm^{-1}) of the aromatic ring in the bio-oil structure was attributed to nicotine, limonene and phenol molecules. The peaks observed at 2960–2870 cm^{-1} in the FT-IR spectrum were attributed to alkane-type compounds (eicosane, pentacosane and octacosane) determined by GC–MS results. As a result, the presence of compounds identified using GC–MS analysis was supported by FT-IR analysis.

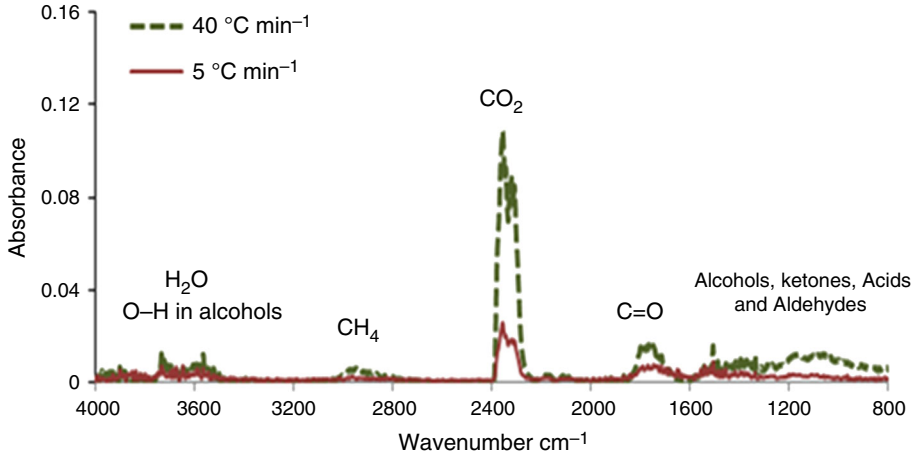

Fig. 7 FT-IR spectra of TW pyrolyzed at 5 and 40 °C min^{-1} at 285 °C, 323 °C

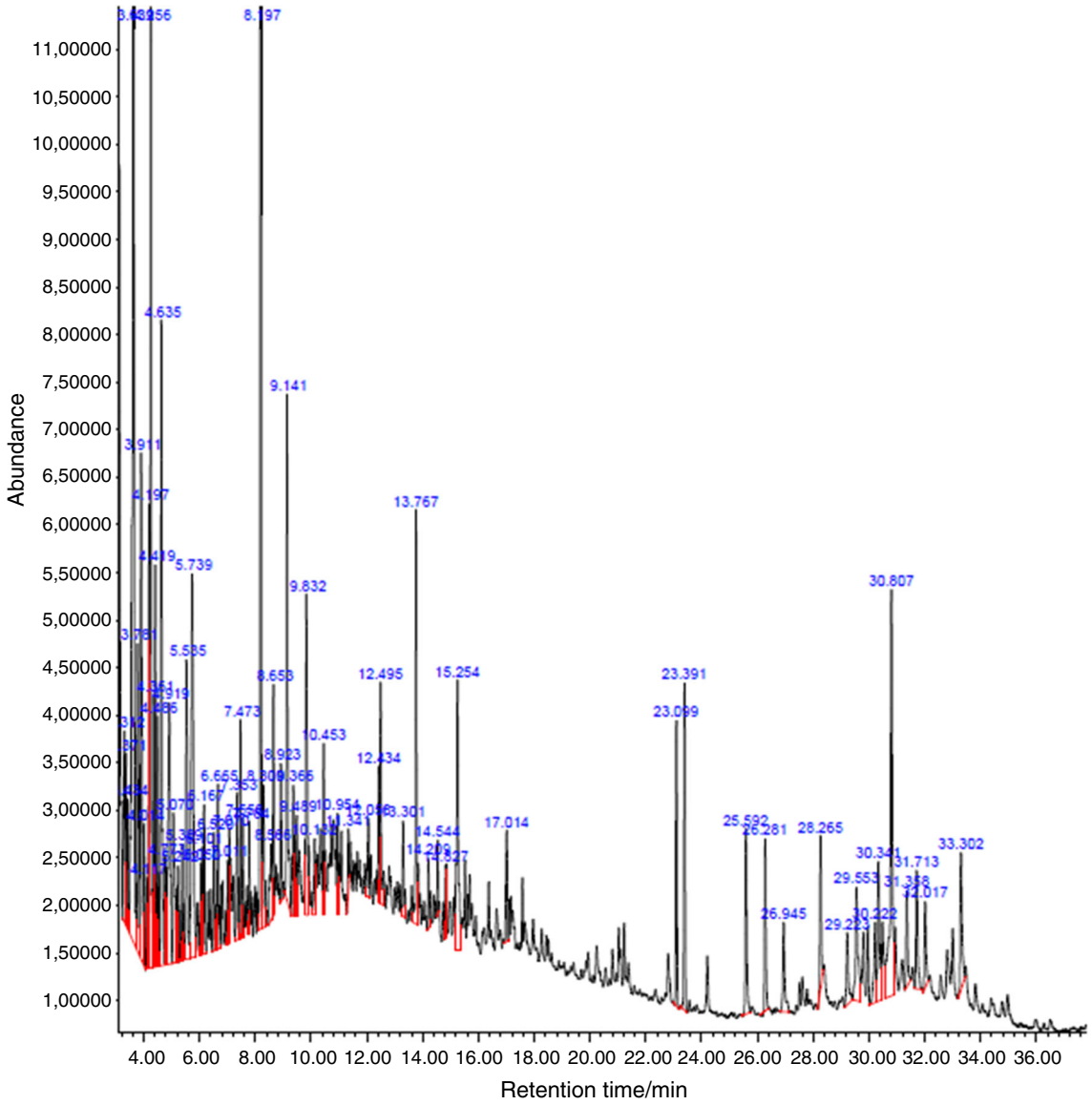

Fig. 8 GC-MS chromatogram of bio-oil obtained TW pyrolyzed at 600 °C for 20 °C min^{-1}

Table 5 Chemical composition of bio-oil obtained at 600 °C for 20 °C min^{-1}

No	Retention time/min	Compounds	Molecular formula	Area/%
1	3.636	Phenol	C_6H_5OH	8.02
2	4.258	Limonene	$C_{10}H_{16}$	4.59
3	4.421	Phenol	C_6H_5OH	1.26
4	4.636	Phenol, p-methylhydroxybenzene	C_6H_5OH, C_7H_8O	2.89
5	4.917	Benzene	C_6H_6	2.06
6	5.532	Phenol, 2,4-dimethylphenol	C_6H_5OH, $C_8H_{10}O$	1.58
7	5.739	Phenol, 4-ethylphenol	C_6H_5OH, $C_8H_{10}O$	3.16
8	8.199	Nicotine	$C_{10}H_{14}N_2$	26.78
9	9.140	Pyridine	C_5H_5N	2.23
10	9.829	Pyridine, nicotyrine	C_5H_5N, $C_{10}H_{10}N_2$	1.52
11	13.769	Neophytadiene	$C_{20}H_{38}$	1.54
12	15.251	Palmitic acid	$C_{16}H_{32}O_2$	1.86
13	23.096	Phenol	C_6H_5OH	1.22
14	23.392	5-Methylorotic acid	$C_6H_6N_2O_4$	1.45
15	29.555	Eicosane	$C_{20}H_{42}$	1.06
16	30.341	Octacosane	$C_{28}H_{58}$	1.01
17	30.807	Pentacosane	$C_{25}H_{52}$	3.33

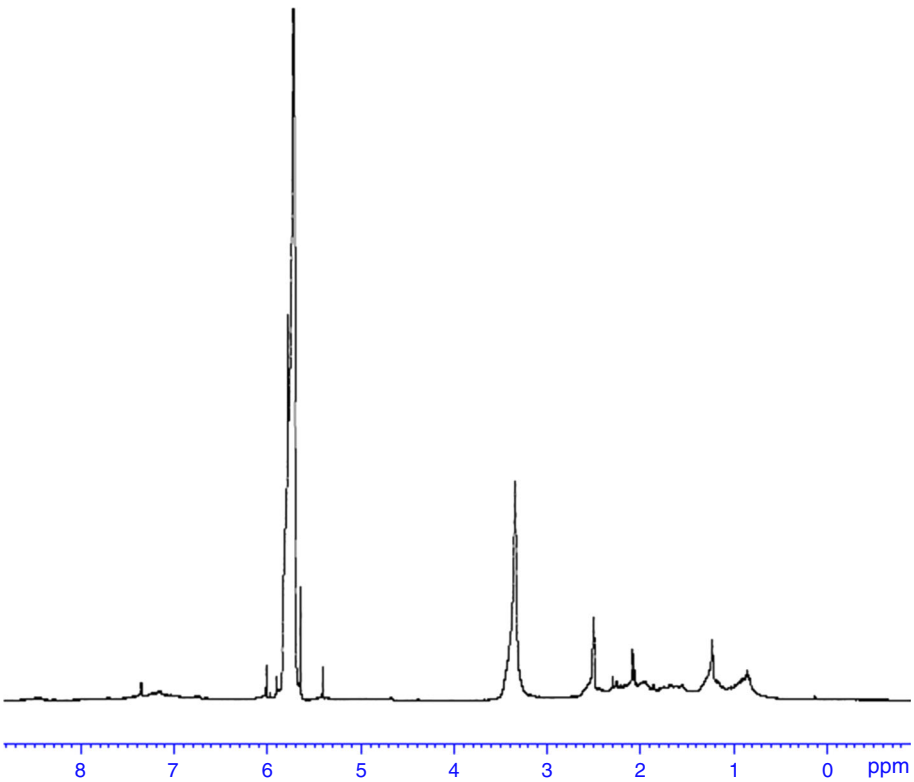

Fig. 9 ^{1}H-NMR spectrum of bio-oil obtained TW pyrolyzed at 600 °C for 20 °C min^{-1}

^{1}H-NMR characterization

In order to better evaluate the compound distribution of the bio-oil obtained from pyrolysis of the tobacco waste, analysis was carried out with ^{1}H NMR technology and the location of the signal groups showed the proton distribution. The ^{1}H NMR spectrum of the bio-oil is shown in Fig. 9. The signals detected at 0.5–1.5 ppm represent aliphatic and aromatic protons bonded to carbon atoms. The next 2–3.0 ppm region corresponded to protons in carbonyl groups (CH_3C=O–, H–C–C=O) and protons in the aromatic ring (CH_3–Ar, –CH_2–Ar, Ar–C–H). Peaks

observed between 0.5 and 3 ppm were confirmed by GC–MS and FT-IR results. The signal observed between 3 and 4 ppm represented protons of aliphatic alcohol (CH_3–O) and heteroatom bound methyl (–CH_3–N) and GC–MS confirmed the presence of the observed nicotine compound with a peak of 26.78% at approximately 8 min. The sharp signal in the 5–6 ppm region corresponds to the proton in the methoxy or phenolic-OH groups [38].

^{1}H-NMR analysis was used to support the presence of phenolic compounds determined by GC–MS results, because FT-IR analysis results were insufficient to determine the presence of phenolic compounds in bio-oil. According to the results of ^{1}H-NMR analysis, the signal observed between 5 and 6 ppm was attributing to the compounds of phenolic-OH groups.

Thus, the presence of phenolic compounds that were difficult to identify with the FT-IR analysis were identified using ^{1}H-NMR analysis. FT-IR analysis and ^{1}H-NMR analysis were used to identify the chemical composition of bio-oil as well as GC–MS analysis, and the results were found to be compatible with each other.

Conclusions

Thermal decomposition of TW was investigated to evaluate its biofuel potential. Thermogravimetric data were used in the analysis of kinetic parameters (E: 201.96–280.38 and k_0: 10^{14}–10^{25}) through the DAEM. The maximum decomposition of TW was occurred at relatively low temperature (320 °C). TG-FT-IR analysis showed that composition and quantity of the evolved gas products effected by temperature and heating rate. Considered the low moisture content and the high volatile matter ratio, thermochemical conversion by pyrolysis was suitable process for TW assessment. According to the results, it was concluded that TW had a potential as a renewable fuel source. For this reason, pyrolysis was carried out with a reaction time of 2 h in the fixed-bed reactor at 600 °C and pyrolysis liquid product was examined. When the GC–MS chromatogram of the liquid product obtained from pyrolysis of the tobacco was examined, it was seen that the nicotine compound with the highest peak area (26.78%). About 3–4 ppm of the methyl protons bound to nitrogen atoms showed the presence of the nicotine compound in the bio-oil structure. At the same time, the aromatic C–H stretching observed at 3040 cm^{-1} in the FT-IR spectrum showed aromatic cyclic compounds were presenting the structure. The nicotine compound was only one of these aromatic ring compounds. As a result, bio-oil produced from the pyrolysis of the tobacco in the waste state could be used as a fuel because of the presence of aliphatic and aromatic hydrocarbons and chemically valuable chemicals (for example, nicotine) had been produced.

Acknowledgements This study is supported by Ondokuz Mayıs University with a project number of PYO.MUH.1911.15.001.

References

1. Wang P, Zhang J, Shao Q, Wang G. Physicochemical properties evolution of chars from palm kernel shell pyrolysis. J Therm Anal Calorim. 2018. https://doi.org/10.1007/s10973-018-7185-z.
2. Tian L, Shen B, Xu H, Li F, Wang Y, Singh S. Thermal behavior of waste tea pyrolysis by TG-FTIR analysis. Energy. 2016;103:533–42.
3. Huang Y-F, Shih C-H, Chiueh P-T, Lo S-L. Microwave co-pyrolysis of sewage sludge and rice straw. Energy. 2015;87:638–44.
4. Guo M, Bi J-C. Characteristics and application of co-pyrolysis of coal/biomass blends with solid heat carrier. Fuel Process Technol. 2015;138:743–9.
5. Soria-Verdugo A, Goos E, García-Hernando N. Effect of the number of TGA curves employed on the biomass pyrolysis kinetics results obtained using the distributed activation energy model. Fuel Process Technol. 2015;134:360–71.
6. Ghouma I, Jeguirim M, Guizani C, Ouederni A, Limousy L. Pyrolysis of olive pomace: degradation kinetics, gaseous analysis and char characterization. Waste Biomass Valoriz. 2017;8:1689–97. https://doi.org/10.1007/s12649-017-9919-8.
7. Viana MM, Rangel BF, Júnior AN, Melchert MBM, Dweck J. Semi-pilot scale sewage sludge pyrolysis and characterization of obtained fractions by thermal analysis. J Therm Anal Calorim. 2016;123:981–91. https://doi.org/10.1007/s10973-015-4821-8.
8. Chiodo V, Zafarana G, Maisano S, Freni S, Urbani F. Pyrolysis of different biomass: direct comparison among Posidonia Oceanica. Lacustrine Alga White-Pine Fuel. 2016;164:220–7.
9. Suriapparao DV, Vinu R. Effects of biomass particle size on slow pyrolysis kinetics and fast pyrolysis product distribution. Waste Biomass Valoriz. 2017. https://doi.org/10.1007/s12649-016-9815-7.
10. Gao W, Chen K, Xiang Z, Yang F, Zeng J, Li J, et al. Kinetic study on pyrolysis of tobacco residues from the cigarette industry. Ind Crops Prod. 2013;44:152–7.
11. Cardoso CR, Ataíde CH. Analytical pyrolysis of tobacco residue: Effect of temperature and inorganic additives. J Anal Appl Pyrolysis. 2013;99:49–57.
12. Yang Z, Zhang S, Liu L, Li X, Chen H, Yang H, et al. Combustion behaviours of tobacco stem in a thermogravimetric analyser and a pilot-scale fluidized bed reactor. Bioresour Technol. 2012;110:595–602.
13. Cardoso CR, Miranda MR, Santos KG, Ataíde CH. Determination of kinetic parameters and analytical pyrolysis of tobacco waste and sorghum bagasse. J Anal Appl Pyrolysis. 2011;92:392–400.
14. Wu W, Mei Y, Zhang L, Liu R, Cai J. Kinetics and reaction chemistry of pyrolysis and combustion of tobacco waste. Fuel. 2015;156:71–80.
15. Chen H, Lin G, Chen Y, Chen W, Yang H. Biomass pyrolytic polygeneration of tobacco waste: product characteristics and Nitrogen transformation. Energy Fuels. 2015;30:1579–88.
16. Wang X, Wang Z, Dai Y, Ma K, Zhu L, Tan H. Thermogravimetric study on the fluecured tobacco leaf pyrolysis and combustion using a distributed activation energy model. Asia-Pac J Chem Eng. 2017;12:75–84.

17. Hossain MM, Scott IM, Berruti F, Briens C. Optimizing pyrolysis reactor operating conditions to increase nicotine recovery from tobacco leaves. J Anal Appl Pyrolysis. 2015;112:80–87.
18. Jiang L, Yuan X, Li H, Xiao Z, Liang J, Wang H, et al. Pyrolysis and combustion kinetics of sludge–camphor pellet thermal decomposition using thermogravimetric analysis. Energy Convers Manag. 2015;106:282–9.
19. Mothé CG, de Miranda IC. Decomposition through pyrolysis process of coconut fiber and rice husk and determination of kinetic parameters according isoconversional methods. J Therm Anal Calorim. 2018;131:601–9. https://doi.org/10.1007/s10973-017-6377-2.
20. Bhavanam A, Sastry RC. Kinetic study of solid waste pyrolysis using distributed activation energy model. Bioresour Technol. 2015;178:126–31.
21. Wang J, Zhao H. Thermogravimetric analysis of rubber glove pyrolysis by different Iso-conversional methods. Waste Biomass Valoriz. 2015;6:527–33. https://doi.org/10.1007/s12649-015-9372-5.
22. Ma Z, Chen D, Gu J, Bao B, Zhang Q. Determination of pyrolysis characteristics and kinetics of palm kernel shell using TGA–FTIR and model-free integral methods. Energy Convers Manag. 2015;89:251–9.
23. Söyler N, Goldfarb JL, Ceylan S, Saçan MT. Renewable fuels from pyrolysis of Dunaliella tertiolecta: an alternative approach to biochemical conversions of microalgae. Energy. 2017;120:907–14.
24. Li H, Xia S, Ma P. Thermogravimetric investigation of the co-combustion between the pyrolysis oil distillation residue and lignite. Bioresour Technol. 2016;218:615–22.
25. Liu G, Song H, Wu J. Thermogravimetric study and kinetic analysis of dried industrial sludge pyrolysis. Waste Manag. 2015;41:128–33.
26. Odeh AO. Oualitative and quantitative ATR-FTIR analysis and its application to coal char of different ranks. J Fuel Chem Technol. 2015;43:129–37.
27. Plis A, Lasek J, Skawińska A, Zuwała J. Thermochemical and kinetic analysis of the pyrolysis process in Cladophora glomerata algae. J Anal Appl Pyrolysis. 2015;115:166–74.
28. Ceylan S, Goldfarb JL. Green tide to green fuels: TG–FTIR analysis and kinetic study of Ulva prolifera pyrolysis. Energy Convers Manag. 2015;101:263–70.
29. Chen Z, Hu M, Zhu X, Guo D, Liu S, Hu Z, et al. Characteristics and kinetic study on pyrolysis of five lignocellulosic biomass via thermogravimetric analysis. Bioresour Technol. 2015;192:441–50.
30. Hu M, Chen Z, Wang S, Guo D, Ma C, Zhou Y, et al. Thermogravimetric kinetics of lignocellulosic biomass slow pyrolysis using distributed activation energy model, Fraser-Suzuki deconvolution, and iso-conversional method. Energy Convers Manag. 2016;118:1–11.
31. Biswas B, Pandey N, Bisht Y, Singh R, Kumar J, Bhaskar T. Pyrolysis of agricultural biomass residues: comparative study of corn cob, wheat straw, rice straw and rice husk. Bioresour Technol. 2017;237:57–63.
32. Song H, Liu G, Wu J. Pyrolysis characteristics and kinetics of low rank coals by distributed activation energy model. Energy Convers Manag. 2016;126:1037–46.
33. Goldfarb JL, Ceylan S. Second-generation sustainability: application of the distributed activation energy model to the pyrolysis of locally sourced biomass–coal blends for use in co-firing scenarios. Fuel. 2015;160:297–308.
34. Zhang Z, He C, Sun T, Zhang Z, Song K, Wu Q, et al. Thermophysical properties of pretreated agricultural residues for biohydrogen production using thermo-gravimetric analysis. Int J Hydrog Energy. 2016;41:5234–42.
35. Wang Z, He Z, Zhao Z, Yi S, Mu J. Influence of ultrasound-assisted extraction on the pyrolysis characteristics and kinetic parameters of eucalyptus. Ultrason Sonochem. 2017;37:47–55.
36. Gómez-Siurana A, Marcilla A, Beltrán M, Berenguer D, Martínez-Castellanos I, Menargues S. TGA/FTIR study of tobacco and glycerol–tobacco mixtures. Thermochim Acta. 2013;573:146–57.
37. Jin W, Shen D, Liu Q, Xiao R. Evaluation of the co-pyrolysis of lignin with plastic polymers by TG-FTIR and Py-GC/MS. Polym Degrad Stab. 2016;133:65–74.
38. Aboulkas A, Hammani H, Achaby M El, Bilal E, Barakat A, harfi K El. Valorization of algal waste via pyrolysis in a fixed-bed reactor: Production and characterization of bio-oil and bio-char. Bioresour Technol. 2017;243:400–8.